

Effect of *N*-Amide Substitution on Antioxidative Activities of Melatonin Derivatives

Panyada Panyatip ^{1,2}, Nutjaree Pratheepawanit Johns ², Aroonsri Priprem ², Kouichi Nakagawa ³, and Ploenthip Puthongking ^{2,*}

¹ Graduate School, Khon Kaen University, Khon Kaen 40002, Thailand; ppanyada90@gmail.com

² Melatonin Research Group, Faculty of Pharmaceutical Sciences, Khon Kaen University, Khon Kaen 40002, Thailand; pnutja@kku.ac.th (N.P.J.); aroonsri@kku.ac.th (A.P.); pploenthip@kku.ac.th (P.P.)

³ Division of Regional Innovation, Graduate School of Health Sciences, Hirosaki University, 66-1 Hon-cho, Hirosaki, Aomori 036-8564, Japan; nakagawa@hirosaki-u.ac.jp

* Correspondence: pploenthip@kku.ac.th; Tel.: +66-43-203149

Received: 22 November 2019; Accepted: 7 January 2020; Published: 8 January 2020

Abstract: Five *N*-amide substituted melatonin (MLT) derivatives were synthesized and evaluated for antioxidative activities, and compounds **9–12** showed higher electron spin resonance (ESR) response than MLT. 4-Bromobenzoyl and naphthoyl derivatives (**10** and **11**) presented stronger hydroxyl radical inhibitory effect than MLT in Fenton reaction. The substitution at the *N*1-position on the MLT core structure with acetyl (**8**), benzoyl (**9**), 4-bromobenzoyl (**10**), and naphthoyl (**11**) and *N*2-substitution with 4-bromobenzoyl (**12**) decreased the reducing power of the derivatives in ferric reducing antioxidant power (FRAP) assay. Compounds **8–11** also presented lower antioxidant capacity than their parent compound in 2,2'-azinobis(3-ethylbenzothiazoline-6-sulfonic acid) disodium salt (ABTS) assay; whereas, compound **12** presented radical scavenging activity similarly to MLT. All aryl derivatives (**9–12**) showed higher ability to quench peroxy radicals than MLT about three times, especially the benzoylated derivatives (**9** and **10**) that presented the highest ability in oxygen radical absorbance capacity (ORAC) assay.

Keywords: melatonin; *N*-amide derivative; radical scavenging; electron spin resonance

1. Introduction

Oxidative stress generates an excess of free radicals that play a vital role in chronic pathological conditions including atherosclerosis, cancer, inflammation and neurodegenerative diseases [1,2]. In the electron transport chain, oxygen (O₂) is involved in mitochondrial generation of energy in the form of ATP. However, some O₂ may escape the chain and be reduced to radicals and non-radical products. Superoxide anion (O₂^{•−}) is one of the radicals formed by the reduction of molecular O₂ through the acceptance of a single electron [3,4]. Superoxide dismutase (SOD) interacts with superoxide to obtain hydrogen peroxide (H₂O₂), an important compound in free radical biochemistry because of its ability to cross cell membranes and break down to produce highly active radicals. Hydroxyl radicals (•OH) are the most reactive and damaging free radicals produced by hydrogen peroxide, particularly in the presence of transition metal ions such as Fe²⁺ and Cu²⁺ [5,6]. The hydroxyl radical can extensively damage different types of molecules, including proteins, nucleic acids, and lipids although it generally interacts with adjacent molecules [7]. The term “antioxidant” can refer to either the compounds that scavenge free radicals produced in the chain reactions or compounds that inhibit the formation of reactive oxidants [8–10]. Therefore, to effectively prevent molecular damage from •OH, an antioxidant should act at the site where the •OH is generated [7].

Among antioxidants, melatonin (*N*-acetyl-5-methoxytryptamine; MLT), a hormone secreted primarily from the pineal gland in the brain, has broad spectrum antioxidant activity, as well as anti-inflammatory activity and a protective effect against neurotoxins [11–14]. As an antioxidant, MLT directly scavenges free radicals such as singlet oxygen ($^1\text{O}_2$), superoxide anion radical ($\text{O}_2^{\bullet-}$), hydrogen peroxide (H_2O_2), hydroxyl radical (OH^\bullet), peroxynitrite anion (ONOO^\bullet), and lipid peroxide radical (LOO^\bullet) [15,16]. MLT also indirectly induces the production of antioxidant enzymes, including glutathione peroxidase, glutathione reductase, glucose-6-phosphate dehydrogenase, and superoxide dismutase, and increases the efficiency of mitochondrial electron transport [3,7]. Unlike other antioxidants, MLT does not undergo redox cycling. Oxidized MLT cannot be reduced to its former state as it forms several stable end-products upon reacting with free radicals [16,17]. In addition, MLT has the ability cross all physiological barriers, e.g., the blood brain barrier, and it is widely distributed in tissues, cells, and subcellular compartments due to its high logP [18,19]. However, many studies have investigated the pharmacokinetics of MLT and found that exogenously administrated MLT displays poor and variable bioavailability (3–56%), which is the consequence of an extensive hepatic first-pass metabolism. The half-life of exogenous MLT is about 12–48 min. Both endogenous and exogenous MLT is primarily metabolized by the cytochrome p450 enzyme CYP1A2. The hepatic enzyme converts MLT to 6-hydroxymelatonin. Then, it is subsequently bound to sulfate and glucuronide and excreted in the urine [20,21].

The rationale for designing the MLT derivatives in this study was retrieved from previous studies of the structure–activity relationship (SAR) of MLT (Figure 1). SAR studies revealed that the indole-core structure (**1**) and 5-methoxy substituted group play a crucial role in its antioxidative properties [22]. The lipophilicity via substitution bulky aromatic at *N*-indole (*N*1) (**2**) improved the antioxidant activity of MLT as shown by thiobarbituric acid reactive substances (TBARS) assay and an acetylated MLT derivative has been reported by our group to be a neuroprotective candidate [23,24]. A 4-bromobenzoyl substituted *N*1-indole derivative (**3**) was shown to be the most active compound in superoxide anion and lipid peroxidation inhibitory assays [25]. In addition, indomethacin, a well-known anti-inflammatory drug, presented 5-methoxyindole core substituted with 4-chlorobenzoyl group at *N*1-position, and it was also used as a prototype for new selective cyclooxygenase-2 (COX-2) inhibitors [26]. Turning to the modification at *N*2-position, hydrazide indole derivatives with halogenated aromatic side chain (**4** and **5**) also presented higher antioxidant activities than MLT [27]. Besides amide and hydrazide groups addition, indole derivatives with lipophilic 3-substituent (**6** and **7**) were designed to mimic the action of anti-inflammatory and analgesic drugs [28]. Therefore, lipophilic MLT derivatives were decided and synthesized in this study. We hypothesized that these derivatives, with lipophilic substitution at *N*1 or *N*2 positions of MLT, would show enhanced antioxidative activities. The scavenging potentials were screened by X-band ESR and then comparatively evaluated by in vitro antioxidant assays such as hydroxyl radicals scavenging test, oxygen radical absorbance capacity (ORAC), 2,2'-azinobis(3-ethylbenzothiazoline-6-sulfonic acid) disodium salt (ABTS) and ferric reducing antioxidant power (FRAP) assays.

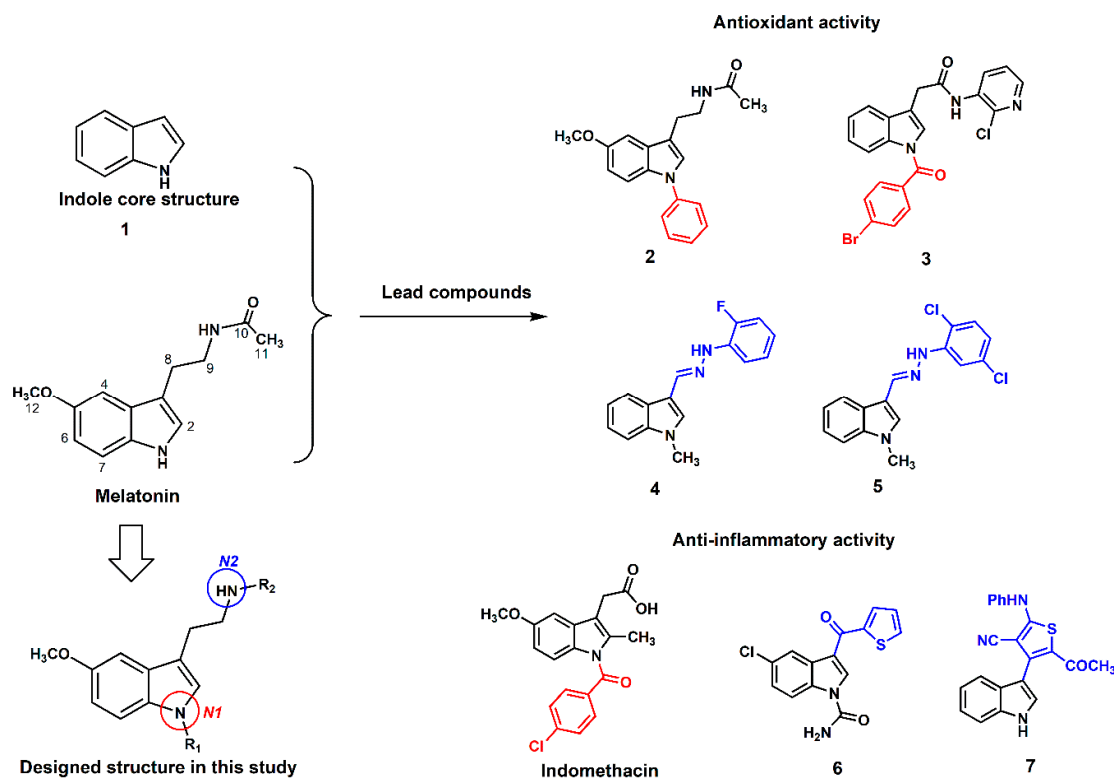


Figure 1. Antioxidant and anti-inflammatory lead compounds relevant to this study [22–28].

2. Materials and Methods

2.1. Chemicals

MLT was purchased from Shanghai Chemical Company (Shanghai, China). 5-methoxytryptamine (5-MT), acetic anhydride, benzoyl chloride, 4-bromobenzoyl chloride, 1-naphthoyl chloride, and 4-dimethylamino pyridine (DMAP) were obtained from Sigma-Aldrich (St. Louis, MO, USA). All commercial solvents were purchased from Modern Chemical Co., Ltd. (Bangkok, Thailand) and distilled prior to use. Column chromatography (CC) was performed on 200–300 mesh silica gel. Thin layer chromatography (TLC) analysis was carried out on pre-coated aluminium sheet 60F₂₅₄ plate (Merck Ltd., Darmstadt, Germany).

2.2. General Procedure for the Preparation of Compounds 8–12

The starting materials for synthesis 8–11 and 12 were MLT and 5-MT, respectively. The synthesis methods are described as following, starting material (1 mmol) was dissolved with dichloromethane (5 mL) in the presence of pyridine (1 mL) and DMAP (0.5 mmol), and five equimolar quantity of corresponding acid chloride was slowly added at 0 °C over 30 min, and resulting solution was stirred at room temperature for 24 h. After the solvent was removed in vacuo, the residue was diluted with water (50 mL) and extracted with ethyl acetate (50 mL×3). The combined extracts were washed with brine (50 mL), dried over Na₂SO₄ anhydrous, and concentrated in vacuo to give the crude extract. Then, it was purified by silica gel column chromatography using an appropriate eluent to give the corresponding purified product.

After purification, all synthetic compounds were elucidated by nuclear magnetic resonance spectroscopy (NMR) (Varian-400 MHz, Palo Alto, CA, USA). The chemical shift (δ) was shown in part per million (ppm) relative to TMS as the internal standard and coupling constant (J) is shown in Hertz (Hz). Deuterated chloroform (CDCl₃) was used as solvent which reference standard for ¹H-NMR and ¹³C-NMR as 7.26 and 77.2 ppm, respectively. Mass spectroscopic (MS) data were

recorded on liquid chromatograph-mass spectrometer (2690, LCT, Waters, Micromass, Wilmslow, UK) with electrospray ionization positive (ESI+) mode. Infrared (IR) spectra were carried out on a Fourier-transform infrared spectrophotometer (Perkin Elmer, Spectrum One, Waltham, MA, USA).

2.2.1. N-(2-(1-acetyl-5-methoxy-1H-indol-3-yl)ethyl)acetamide (8)

Pale yellowish solid, 126.2 mg (46%). R_f = 0.3 (100% EtOAc); IR (KBr) 3260, 3085, 2940, 1712 cm^{-1} ; ^1H NMR (CDCl_3 , 400 MHz) δ : 7.16 (s, 1H), 6.93 (d, J = 1.8 Hz, 1H), 6.89 (dd, J = 1.8, 9.0 Hz, 1H), 6.20 (s, 1H), 3.81 (s, 3H), 3.54 (q, J = 6.6 Hz, 2H), 2.83 (t, J = 6.6 Hz, 2H), 2.44 (s, 3H), 1.93 (s, 3H); ^{13}C NMR (CDCl_3 , 100 MHz) δ : 170.4, 168.1, 156.6, 131.6, 130.6, 123.3, 119.6, 117.5, 113.4, 102.0, 55.8, 39.0, 25.3, 23.6, 23.3. HR-ESI-MS m/z : 275.1394 ($\text{M}+\text{H}^+$, Calcd for $\text{C}_{15}\text{H}_{18}\text{N}_2\text{O}_3$, 275.1395).

2.2.2. N-(2-(1-benzoyl-5-methoxy-1H-indol-3-yl)ethyl)acetamide (9)

Yellowish solid, 117.7 mg (35%), R_f = 0.6 (EtOAc:*n*-Hexane, 1:1). IR (KBr) 3336, 3052, 2918, 1697 cm^{-1} ; ^1H NMR (CDCl_3 , 400 MHz) δ : 7.44–7.50 (m, 1H), 7.30–7.37 (m, 4H), 7.21 (d, J = 9.3 Hz, 1H), 6.92 (d, J = 2.0 Hz, 1H), 6.82 (dd, J = 2.0, 9.3 Hz, 1H), 6.80 (s, 1H), 4.07 (t, J = 7.3 Hz, 2H), 3.75 (s, 3H), 3.03 (t, J = 7.3 Hz, 2H), 2.21 (s, 3H); ^{13}C NMR (CDCl_3 , 100 MHz) δ : 174.5, 173.4, 154.0, 135.4, 131.3, 128.5, 128.2, 127.7, 123.4, 112.6, 112.1, 111.8, 100.2, 55.8, 47.0, 29.7, 26.1, 24.9. HR-ESI-MS m/z : 337.1552 ($\text{M}+\text{H}^+$, Calcd for $\text{C}_{20}\text{H}_{20}\text{N}_2\text{O}_3$, 337.1552).

2.2.3. N-(2-(1-4-bromobenzoyl-5-methoxy-1H-indol-3-yl)ethyl)acetamide (10)

Pale yellowish solid, 49.8 mg (12% yield), R_f = 0.7 (EtOAc:*n*-Hexane, 1:1). IR (KBr) 3545, 2940, 2865, 2732, 1702, 1454, 1389, 1377 cm^{-1} ; ^1H NMR (CDCl_3 , 400 MHz) δ : 7.41 (d, J = 8.5 Hz, 2H), 7.22 (d, J = 8.8 Hz, 1H), 7.08 (d, J = 8.5 Hz, 2H), 6.91 (d, J = 2.3 Hz, 1H), 6.83 (dd, J = 2.3, 8.8 Hz, 1H), 6.72 (d, J = 2.2 Hz, 1H), 4.05 (t, J = 7.0 Hz, 2H), 3.76 (s, 3H), 3.02 (t, J = 7.0 Hz, 2H), 2.23 (s, 3H); ^{13}C NMR (CDCl_3 , 100 MHz) δ : 173.5, 173.4, 154.1, 134.0, 131.9, 131.7, 129.6, 127.7, 126.7, 123.7, 112.4, 111.9, 111.8, 100.2, 55.7, 47.0, 26.0, 25.0. HR-ESI-MS m/z : 437.0477 ($\text{M}+\text{Na}^+$, Calcd for $\text{C}_{20}\text{H}_{19}\text{BrN}_2\text{O}_3\text{Na}$, 437.0477).

2.2.4. N-(2-(1-naphthoyl-5-methoxy-1H-indol-3-yl)ethyl)acetamide (11)

Off-white solid, 81.2 mg (21%), R_f = 0.7 (EtOAc:*n*-Hexane, 1:1). IR (KBr) 3398, 2900–3000, 1679 cm^{-1} ; ^1H NMR (CDCl_3 , 400 MHz) δ : 7.84 (d, J = 8.3 Hz, 1H), 7.74–7.81 (m, 3H), 7.59 (t, J = 7.3 Hz, 1H), 7.53 (t, J = 7.3 Hz, 1H), 7.40 (d, J = 8.3 Hz, 1H), 7.20 (d, J = 8.8 Hz, 1H), 6.93 (s, 1H), 6.75 (dd, J = 1.7, 8.8 Hz, 1H), 6.69 (s, 1H), 4.15 (t, J = 7.2 Hz, 2H), 3.47 (s, 3H), 3.08 (t, J = 7.2 Hz, 2H), 2.23 (s, 3H); ^{13}C NMR (CDCl_3 , 100 MHz) δ : 174.8, 173.7, 154.2, 129.4, 129.3, 128.6, 128.4, 127.9, 127.1, 124.4, 112.8, 112.3, 111.9, 100.2, 55.6, 47.3, 26.4, 25.1. HR-ESI-MS m/z : 409.1527 ($\text{M}+\text{Na}^+$, Calcd for $\text{C}_{24}\text{H}_{22}\text{N}_2\text{O}_3\text{Na}$, 409.1528).

2.2.5. 4-bromo-N-(2-(5-methoxy-1H-indol-3-yl)ethyl)benzamide (12)

Off-white solid, 276.2 mg (74%), R_f = 0.5 (EtOAc:*n*-Hexane, 1:1). IR (KBr) 3390, 3311, 3079, 2924, 1638 cm^{-1} ; ^1H NMR (CDCl_3 , 400 MHz) δ : 7.45–7.56 (m, 4H), 7.25 (d, J = 8.8 Hz, 1H), 7.03 (d, J = 2.3 Hz, 1H), 7.01 (d, J = 2.1 Hz, 1H), 6.87 (dd, J = 2.3, 8.8 Hz, 1H), 3.78 (s, 3H), 3.75 (t, J = 6.4 Hz, 2H), 3.04 (t, J = 6.4 Hz, 2H); ^{13}C NMR (CDCl_3 , 100 MHz) δ : 166.6, 154.2, 133.5, 131.8, 131.7, 128.6, 126.1, 123.0, 112.7, 112.6, 112.3, 100.6, 56.0, 40.6, 25.3. HR-ESI-MS m/z : 395.0370 ($\text{M}+\text{Na}^+$, Calcd for $\text{C}_{18}\text{H}_{17}\text{BrN}_2\text{O}_2\text{Na}$, 395.0371).

2.3. Electron Spin Resonance (ESR) Study

MLT and 5-MT were used as the reference samples. The samples (approximately 5 mg) were filled into the glass capillary (outer diameter, 1.0 mm; inner diameter, 0.9 mm), and the end of each tube was closed with clay. Then samples were transferred to an ESR quartz tube (JOEL Co. Ltd., Tokyo, Japan). The X-band (9 GHz) ESR/EPR spectrometer (JOEL RE3X, Tokyo, Japan) was used for ESR measurement. The ESR conditions were composed of microwave power 5 mW, time constant

0.1 s, sweep time 1 min for screening phase and 4 min for analysis, magnetic field modulation 0.32 mT, and sweep width 10 mT. All ESR spectra were obtained from a single scan. The measurement was performed at room temperature [29]. The hydroxyl radical scavenging test was performed at room temperature. The radicals were generated by the Fenton reaction. 5,5-Dimethyl N-oxide pyrroline (DMPO) was used as the nitron spin trap. ESR spectra were recorded after 50 μ L of phosphate buffer solution (PBS) pH 7.4 or the sample at the final concentration of 25 μ M was mixed with iron (II) sulfate solution (2 mM, 25 μ L) DMPO (150 mM, 50 μ L). Hydrogen peroxide (30%, 25 μ L) was added to initiate the reaction [30]. The resultant of DMPO-OH adduct was measured by ESR technique under the following conditions: center field, 336.5 mT; sweep width, 5 mT; modulation frequency, 100 kHz; modulation width, 0.32 mT; amplitude, 1×10^3 ; sweep time, 2 min; time constant, 0.1 s; microwave power, 10.0 mW; and microwave frequency, 9.44 GHz. The percentage of all compounds were calculated using Equation (1).

$$\text{Percentage of Amplitude} = \frac{A_s}{A_{\text{PBS}}} \times 100, \quad (1)$$

where A_s was signal amplitude of tested compounds and A_{PBS} was signal amplitude of PBS.

2.4. Study of Antioxidant Activities

2.4.1. 2,2'-azinobis(3-ethylbenzothiazoline-6-sulfonic acid) disodium salt (ABTS) assay.

ABTS solution was prepared by mixing of 5 mL of 7 μ M ABTS stock solution with 88 μ L of 140 μ M potassium persulfate ($\text{K}_2\text{S}_2\text{O}_8$) and kept in the dark for 16 h. Next, 100 μ L of ABTS solution was mixed with 100 μ L of the sample in various concentrations in 96-well plates and left for 6 min. Ethanol was used as blank. The absorbance was measured at wavelength 700 nm [31]. Trolox was used as a standard.

2.4.2. Oxygen Radical Absorbance Capacity (ORAC) assay

One hundred and fifty microliters of fluorescein and 25 μ L of the sample solutions (1 μ M) were added into 96-well plates. The mixture was incubated for 15 min at 37 $^{\circ}\text{C}$. Then, 60 μ L of 2,2'-azobis(2-methylpropionamide) dihydrochloride (AAPH) solution was added rapidly. The fluorescence was recorded every minute for 120 min at the excitation wavelength 485 nm and emission wavelength 538 nm [32]. Trolox solutions in various concentrations (0.13–6.25 μ M) were used for calibration curve between area under the curve (AUC) and trolox concentrations. Trolox equivalent antioxidant capacity (TEAC) values was calculated from Equation (2).

$$y = 34,473.40x + 54,457.96, \quad (2)$$

where y was area under the curve (AUC) and x was trolox concentration (μ M).

2.4.3. Ferric Reducing Antioxidant Power (FRAP) Assay

Reducing ability of the compounds was determined by a modified ferric reducing antioxidant power (FRAP) method [33]. FRAP reagent was prepared by mixing of 300 mM acetate buffer (pH 3.6) with 20 mM ferric chloride solution and 10 mM 2,4,6-Tris(2-pyridyl)-1,3,5-triazine (TPTZ) solution in the ratio 10:1:1 and incubated at 37 $^{\circ}\text{C}$ for 30 min. Then, 150 μ L of FRAP reagent was pipetted into 96-well plates. After that, 50 μ L of the sample was added, and after 5 min, the absorbance was measured at wavelength 595 nm. In order to calculate TEAC values, trolox was used as standard.

2.5. Statistical Analysis

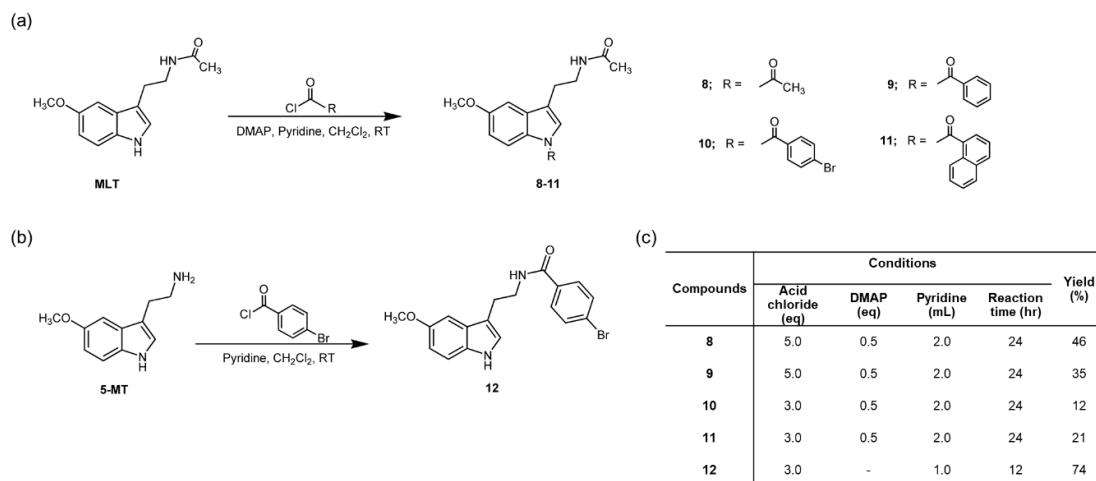
Data was shown as mean and standard deviation (mean \pm SD). The data was analyzed by using Statistical Product and Service Solution (SPSS) software version 19.0 (SPSS Inc., Chicago, IL, USA).

Differences between experimental groups were analyzed by one-way analysis of variance. All differences were considered significant only when the p-value was less than 0.05.

3. Results and Discussion

3.1. Chemistry

N-amide MLT derivatives (8–12) were synthesized as shown in Scheme 1. The structures of all compounds were elucidated and confirmed by IR, Mass, and NMR measurements as shown in sections 2.2.1–2.2.5.



Scheme 1. The proposed reactions and structure of *N*-amide melatonin (MLT) derivatives in this study. (a) Compounds 8–11, (b) compound 12, and (c) conditions.

The assignment of **8** presented the core MLT signals of methyl protons at δ 1.93 and 3.81 ppm. The signals of methylene protons showed the triplet pattern at δ 2.83 ppm (J = 6.6 Hz) and 3.54 ppm (J = 6.6 Hz). Methine protons of 2- and 4-positions of the compound showed singlet pattern at δ 26.20 and 7.16 ppm. Methine protons of 6- and 7-positions presented the doublet of doublet pattern at δ 6.89 ppm (J = 1.8 and 9.0 Hz) and doublet pattern at δ 6.93 ppm (J = 1.8 Hz), respectively. The additional singlet pattern signal of methyl proton at δ 2.44 ppm, methyl carbon signal at δ 23.3 ppm, and quaternary carbonyl carbon signal at δ 168.2 ppm indicated the presence of acetyl moiety in **8**. For compound **9**, the aromatic protons on additional benzoyl group presented the signals at δ 7.30–7.37 and 7.44–7.50 ppm as multiplet pattern. Moreover, methine carbons also presented the signals at δ 128.2, 128.5, and 131.3 ppm on ^{13}C -NMR spectrum. Quaternary and carbonyl carbons of benzoyl moiety showed the signals at δ 135.4 and 173.4 ppm, respectively. The additional aromatic protons of 4-bromobenzoyl moiety on compound **10** showed two doublet signals at δ 7.08 and 7.41 ppm (J = 8.5 Hz). Methine carbons presented the signals at δ 129.6 and 131.7 ppm, consequently. In addition, the additional signals of quaternary carbons also presented at δ 126.7, 134.0, and 173.4 ppm, respectively. The naphthoyl group of compound **11** presented the extra signals at δ 7.74–7.81 ppm as multiplet pattern and the aromatic carbons also showed the signals at δ 124.4, 127.1, 127.9, 128.4, 128.6, 129.3, and 129.4 ppm, consequently. The methylene protons of compound **12** presented the triplet signals at δ 3.04 ppm (J = 6.4 Hz) and 3.75 ppm (J = 6.4 Hz). The aromatic protons of the additional 4-bromobenzoyl group presented the signal at δ 7.48–7.56 ppm as multiplet pattern and carbon signals at δ 128.6 and 131.8 ppm. And the signals of quaternary carbons appeared at δ 126.1, 133.5, and 166.6 ppm.

3.2. Electron Spin Resonance (ESR) Study

The MLT derivatives presented similar ESR patterns when compared with MLT and 5-MT spectra (Figure 2). Derivatives 9–12, which are aromatic substituent derivatives, had a higher response than their parent compounds; however, 8 had a lower intensity. The spectral pattern for 9 differed from others, which suggested that the location of the unpaired electron in 9 differed from others. These phenomena indicated that derivatives 9–12 would become their radical forms more readily than MLT and 5-MT.

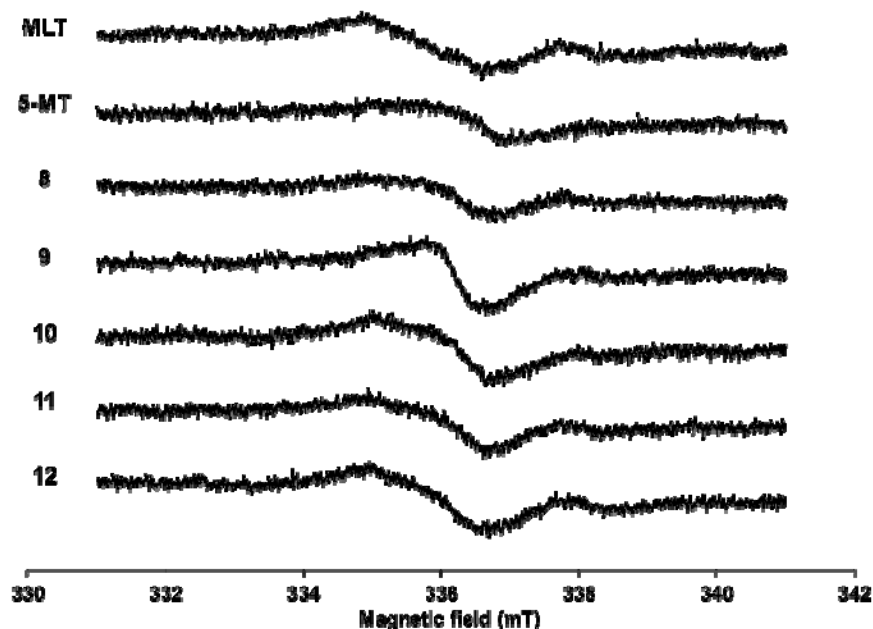


Figure 2. ESR spectra of MLT, 5-MT, and 9–13 at a 10 mT sweep width.

The spectra of DMPO spin trapping of hydroxyl radicals were presented in Figure 3. The DMPO-OH adduct was easily distinguished by a typical 4-line spectrum with the relative intensity ratio 1:2:2:1 due to the equivalent hyperfine splitting constants [34]. Although MLT is the powerful antioxidant, it slightly inhibited the Fenton reaction at concentration of 25 μM compared with PBS. The relative attenuation of the ESR signal amplitude of MLT was 6.19%. From previous report [27], the biphasic pattern of MLT scavenging activity was found. At low concentration (1 μM) and high concentration (500–1,000 μM) had higher effect, whereas lower effect presented in between concentration (10–100 μM) in H_2O_2 -induced membrane lipid peroxidation experiment. At the same concentration, compounds 10 and 11 showed the lowest intensity among other derivatives with the relative attenuation of the ESR signal amplitude were 22.12% and 24.78%, respectively. Substitution with 4-bromobenzoyl and naphthoyl groups at *N1*-position (10 and 11) obtained compounds with a stronger hydroxyl radical inhibitory effect than MLT.

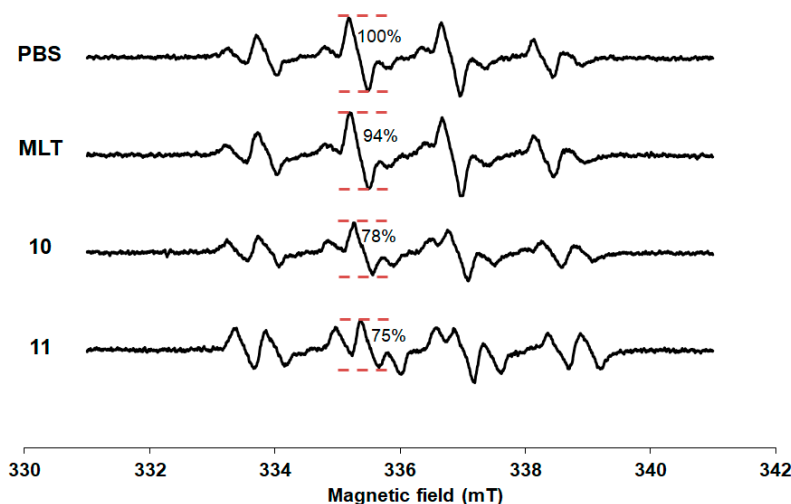


Figure 3. ESR spectra of spin adduct of hydroxyl radical observed in Fenton reaction.

3.3. Study of Antioxidant Activities

ABTS radical scavenging assay is based on the electron transfer (ET) mechanism. The ABTS^+ radical cation would be scavenged by the electron donating of antioxidants in the reaction mixture [16,35]. The antioxidant capacities of all compounds in ABTS assay were shown as the half maximal inhibitory concentration (IC_{50}) value. The *N1*-substituted derivatives (compounds 8–11) presented significantly lower activity than their parent (MLT) and the standard antioxidant (trolox) (Figure 4a). Whereas, the *N2*-substituted derivative (12) did not show statistically different capacity from MLT and 5-MT. Comparing between *N1* and *N2*-substituted compounds, the compounds without substituted *N1*-position, such as MLT, 5-MT, and compound 12, exhibited more potent activity than the *N1*-substituted derivatives (8–11). According with the report of Tan and colleagues [36] which proposed a chemical mechanism for MLT interaction with ABTS^+ radicals. MLT inhibited the radicals by donating an electron at *N1*-indole position to ABTS^+ radical and forming melatonyl radical cation and melatonyl neutral radical, respectively. To scavenge additional ABTS^+ radicals, the neutral radical would interact with ABTS^+ radical to form cyclic 3-hydroxymelatonin (3-OHM), then, scavenged two ABTS^+ radicals and formed the final metabolite acetyl-*N*-formyl-5-methoxykynurenamine (AFMK). Therefore, the substitution of *N1*-position with more lipophilic groups (8–11) affected the scavenging abilities of MLT derivatives by hindering the interaction between the derivatives and radicals. While, the *N2*-substitution (12) had no effect on the scavenging ability as no significant difference when compared to MLT and its parent compound.

The study of hydrogen atom transfer (HAT) ability was determined in the ORAC assay. All compounds were also tested at 1 μM . The peroxy radicals were produced by decomposition of AAPH and caused the decrease of fluorescent intensity in the test solution [37]. From TEAC values, MLT presented twice the active quenching ability of trolox as shown in Figure 4b corresponded to the Pieri's report [38]. Comparing between 5-MT and MLT, the effect of acetylated substitution at *N2*-position increased the scavenging ability by about four times. Interestingly, the addition of halogenated aromatic at *N2*-position (12) highly increased the quenching ability than its parent compound and MLT. As Tan [39] mentioned earlier, the present of *N*-acetyl side chain on MLT structure would produce a synergistic action against free radicals. For *N1*-substituted derivatives, all lipophilic derivatives (9, 10, and 11) enhanced peroxy radical scavenging activity compared with MLT and trolox. From these findings, it could be suggested that lipophilic substitution at either the *N1* or *N2*-positions enhanced the scavenging of peroxy radical.

The reducing ability of all compounds were tested in FRAP assay at 1 μM . All compounds presented lower activity than trolox ($\text{TEAC} < 1.00$), as shown in Figure 4c. Moreover, all derivatives exhibited lower activity than their parent compounds. As same as the result from ABTS assay, it

could be assumed that the addition of more lipophilic groups would decrease the reducing power of the derivatives owing to more difficult electron transfer from the nitrogen atom of the derivatives to the Fe(III)TPTZ complex.

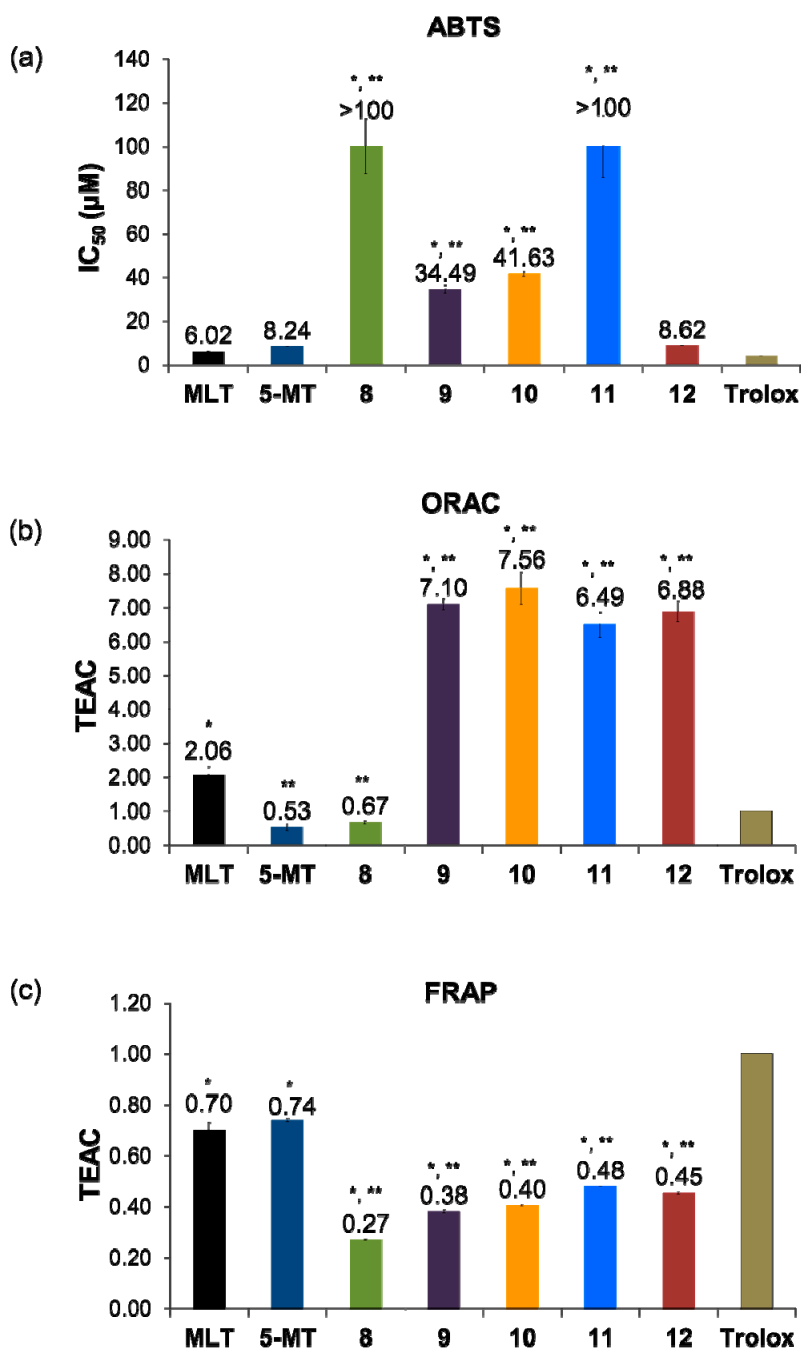


Figure 4. The antioxidant capacities of MLT and its derivatives on (a) ABTS, (b) ORAC, and (c) FRAP assays. Data represented mean \pm SD ($n = 3$). * $p < 0.05$ compared with trolox, ** $p < 0.05$ compared with MLT.

4. Conclusions

In conclusion, we synthesized a series of five MLT derivatives and evaluated them for ESR screening and in vitro antioxidative activities. The evaluation of the antioxidant activities of these compounds revealed that the modification of MLT structure by addition of lipophilic groups

probably hindered the electron transfer ability and reducing power of the compounds, for instance, the *N*1-substituted derivatives (**8–11**) presented lower activity than MLT in both the ABTS and FRAP assays. However, aromatic substituent derivatives presented their potentialities to inhibit hydroxyl radical which the most reactive radical. Particularly, naphthoylated and 4-bromobenzoylated derivatives (**11** and **10**) were the most effective compounds to inhibit the Fenton reaction in ESR study. The addition of aryl groups (**9–12**) enhanced the peroxy radical quenching abilities of the compounds about three times that of MLT, especially for the benzoylated derivatives (**9** and **10**) in the ORAC assay. Interestingly, 4-bromobenzoylated MLT (**10**) exhibited its antioxidant ability against most reactive radical as hydroxyl radicals and the membrane damaging radical as peroxy radicals. *N*1-substitution with halogenated aromatic is remarkable for designing MLT derivatives in further study. In addition, these derivatives would be investigated other pharmacological activities that involved free radicals and their pharmacokinetics in our ongoing study.

Author Contributions: Conceptualization, P.P.(Ploenthip Puthongking); methodology, P.P.(Ploenthip Puthongking); formal analysis, P.P.(Ploenthip Puthongking) and P.P.(Panyada Panyatip); investigation, P.P.(Ploenthip Puthongking), A.P. and K.N.; resources, P.P.(Ploenthip Puthongking), K.N. and P.P.(Panyada Panyatip); writing—original draft preparation, P.P.(Ploenthip Puthongking) and P.P.(Panyada Panyatip); writing—review and editing, P.P.(Ploenthip Puthongking), P.P.(Panyada Panyatip), K.N., A.P. N.P.J.; visualization, P.P.(Ploenthip Puthongking), N.P.J., A.P.; supervision, P.P.(Ploenthip Puthongking), N.P.J., A.P.; project administration, P.P.(Ploenthip Puthongking); funding acquisition P.P.(Ploenthip Puthongking). All authors have read and agreed to the published version of the manuscript.

Funding: This research was funded by the Graduate Research Fund Academic Year 2019 from the National Research Council of Thailand (NRCT), the Office of the Higher Education Commission (Total Synthesis of Melatonin Project), and the Thailand Research Fund (DBG6080006), Thailand.

Acknowledgments: The authors thank the Graduate School and the Faculty of Pharmaceutical Sciences, Khon Kaen University for their facilities and Dr. Glenn Borlace, Faculty of Pharmaceutical Sciences, Khon Kaen University for English language assistance.

Conflicts of Interest: The authors declare that there are no conflicts of interest.

References

1. Poprac, P.; Jomova, K.; Simunkova, M.; Kollar, V.; Rhodes, C.J.; Valko, M. Targeting free radicals in oxidative stress-related human diseases. *Trends Pharm. Sci.* **2017**, *38*, 592–607.
2. Gupta, P.; Jyoti, R.B.; Gupta, S. Free radical pharmacology and its role in various diseases. *J. Drug Deliv.* **2019**, *9*, 690–694.
3. Acuña-Castroviejo, D.; Martín, M.; Macías, M.; Escames, G.; León, J.; Khaldy, H.; Reiter, R.J. Melatonin, mitochondria, and cellular bioenergetics. *J. Pineal Res.* **2001**, *30*, 65–74.
4. Davies, M.J. Quantification and Mechanisms of Oxidative Stress in Chronic Disease. *Proceedings* **2019**, *11*, 18.
5. Cheeseman, K.H.; Slater, T.F. An introduction to free radical biochemistry. *Br. Med. Bull.* **1993**, *49*, 481–493.
6. Cui, K.; Luo, X.; Xu, K.; Murthy, M.V. Role of oxidative stress in neurodegeneration: Recent developments in assay methods for oxidative stress and nutraceutical antioxidants. *Prog. Neuropsychopharmacol. Biol. Psychiatry* **2004**, *28*, 771–799.
7. Reiter, R.J.; Tan, D.X.; Burkhardt, S. Reactive oxygen and nitrogen species and cellular and organismal decline: Amelioration with melatonin. *Mech. Ageing Dev.* **2002**, *123*, 1007–1019.
8. Sisein, E.A. Biochemistry of free radicals and antioxidants. *Sch. Acad. J. Biosci.* **2014**, *2*, 110–118.
9. Neha, K.; Haider, M.R.; Pathak, A.; Yar, M.S. Medicinal prospects of antioxidants: A review. *Eur. J. Med. Chem.* **2019**, *178*, 687–704.
10. Huang, D.; Ou, B.; Prior, R.L. The chemistry behind antioxidant capacity assays. *J. Agric. Food Chem.* **2005**, *53*, 1841–1856.
11. Tan, D.X.; Manchester, L.C.; Terron, M.P.; Flores, L.J.; Tamura, H.; Reiter, R.J. Melatonin as a naturally occurring co-substrate of quinone reductase-2, the putative MT3 melatonin membrane receptor: Hypothesis and significance. *J. Pineal Res.* **2007**, *43*, 317–320.
12. Paradies, G.; Petrosillo, G.; Paradies, V.; Reiter, R.J.; Ruggiero, F.M. Melatonin, cardiolipin and mitochondrial bioenergetics in health and disease. *J. Pineal Res.* **2010**, *48*, 297–310.

13. Tan, D.X.; Manchester, L.; Qin, L.; Reiter, R. Melatonin: A mitochondrial targeting molecule involving mitochondrial protection and dynamics. *Int. J. Mol. Sci.* **2016**, *17*, 2124.
14. Cardinali, D.P. Melatonin: Clinical perspectives in neurodegeneration. *Front Endocrinol.* **2019**, *10*, 480.
15. Tomás-Zapico, C.; Coto-Montes, A. A proposed mechanism to explain the stimulatory effect of melatonin on antioxidative enzymes. *J. Pineal Res.* **2005**, *39*, 99–104.
16. Galano, A.; Reiter, R.J. Melatonin and its metabolites vs oxidative stress: From individual actions to collective protection. *J. Pineal Res.* **2018**, *65*, 12514.
17. Tan, D.X.; Manchester, L.C.; Reiter, R.J.; Qi, W.B.; Karbownik, M.; Calvo, J.R. Significance of melatonin in antioxidative defense system: Reactions and products. *Neurosignals* **2000**, *9*, 137–159.
18. Harpsøe, N.G.; Andersen, L.P.H.; Gögenur, I.; Rosenberg, J. Clinical pharmacokinetics of melatonin: A systematic review. *Eur. J. Clin. Pharm.* **2015**, *71*, 901–909.
19. Salehi, B.; Sharopov, F.; Fokou, P.V.T.; Kobylinska, A.; Jonge, L.D.; Tadio, K.; Iriti, M. Melatonin in Medicinal and Food Plants: Occurrence, Bioavailability, and Health Potential for Humans. *Cells* **2019**, *8*, 681.
20. Zetner, D.; Andersen, L.P.H.; Rosenberg, J. Pharmacokinetics of alternative administration routes of melatonin: A systematic review. *Drug Res.* **2016**, *66*, 169–173.
21. Farzaei, M.H.; Hajialyani, M.; Naseri, R. Melatonin. In *Nonvitamin and Nonmineral Nutritional Supplements*; Nabavi, S.M., Silva, A.S.; Academic Press: Cambridge, MA, USA, **2019**; pp. 99–105.
22. Gozzo, A.; Lesieur, D.; Duriez, P.; Fruchart, J.C.; Teissier, E. Structure-activity relationships in a series of melatonin analogues with the low-density lipoprotein oxidation model. *Free Radic. Biol. Med.* **1999**, *26*, 1538–1543.
23. Mor, M.; Silva, C.; Vacondio, F.; Plazzi, P.V.; Bertoni, S.; Spadoni, G.; Franceschini, D. Indole-based analogs of melatonin: In vitro antioxidant and cytoprotective activities. *J. Pineal Res.* **2004**, *36*, 95–102.
24. Panyatip, P.; Puthongking, P.; Tadtong, S. Neuroprotective and neuritogenic activities of melatonin and N-acetyl substituent derivative. *Isan J. Pharm. Sci.* **2015**, *11*, 14–19.
25. Oelgen, S.; Çoban, T. Synthesis and antioxidant properties of novel N-Substituted indole-2-carboxamide and indole-3-acetamide derivatives. *Arch. Pharm.* **2002**, *335*, 331–338.
26. Kalgutkar, A.S.; Marnett, A.B.; Crews, B.C.; Remmel, R.P.; Marnett, L.J. Ester and amide derivatives of the nonsteroidal antiinflammatory drug, indomethacin, as selective cyclooxygenase-2 inhibitors. *J. Med. Chem.* **2000**, *43*, 2860–2870.
27. Shirinzadeh, H.; Eren, B.; Gurer-Orhan, H.; Suzen, S.; Özden, S. Novel indole-based analogs of melatonin: Synthesis and in vitro antioxidant activity studies. *Molecules* **2010**, *15*, 2187–2202.
28. Radwan, M.A.; Ragab, E.A.; Sabry, N.M.; El-Shenawy, S.M. Synthesis and biological evaluation of new 3-substituted indole derivatives as potential anti-inflammatory and analgesic agents. *Bioorg. Med. Chem.* **2007**, *15*, 3832–3841.
29. Nakagawa, K. Electron spin resonance investigation of small spin probes in aqueous and vesicle phases of mixed membranes made from poly (oxyethylene) hydrogenated castor oil and hexadecane. *Lipids* **2005**, *40*, 745.
30. Trouillas, P.; Calliste, C.A.; Allais, D.P.; Simon, A.; Marfak, A.; Delage, C.; Duroux, J.L. Antioxidant, anti-inflammatory and antiproliferative properties of sixteen water plant extracts used in the Limousin countryside as herbal teas. *Food Chem.* **2003**, *80*, 399–407.
31. Re, R.; Pellegrini, N.; Proteggente, A.; Pannala, A.; Yang, M.; Rice-Evans, C. Antioxidant activity applying an improved ABTS radical cation decolorization assay. *Free Radic. Biol. Med.* **1999**, *26*, 1231–1237.
32. Ou, B.; Hampsch-Woodill, M.; Prior, R.L. Development and validation of an improved oxygen radical absorbance capacity assay using fluorescein as the fluorescent probe. *J. Agric. Food Chem.* **2001**, *49*, 4619–4626.
33. Iqbal, S.; Younas, U.; Chan, K.W.; Sarfraz, R.A.; Uddin, M.K. Proximate composition and antioxidant potential of leaves from three varieties of Mulberry (*Morus* sp.): A comparative study. *Int. J. Mol. Sci.* **2012**, *13*, 6651–6664.
34. Rohn, S.; Kroh, L.W. Electron spin resonance-a spectroscopic method for determining the antioxidative activity. *Mol. Nutr. Food Res.* **2005**, *49*, 898–907.
35. Zulueta, A.; Esteve, M.J.; Frigola, A. ORAC and TEAC assays comparison to measure the antioxidant capacity of food products. *Food Chem.* **2009**, *114*, 310–316.

36. Tan, D.X.; Hardeland, R.; Manchester, L.C.; Poeggeler, B.; Lopez-Burillo, S.; Mayo, J.C.; Reiter, R.J. Mechanistic and comparative studies of melatonin and classic antioxidants in terms of their interactions with the ABTS cation radical. *J. Pineal Res.* **2003**, *34*, 249–259.
37. Ou, B.; Chang, T.; Huang, D.; Prior, R.L. Determination of total antioxidant capacity by oxygen radical absorbance capacity (ORAC) using fluorescein as the fluorescence probe: First action 2012.23. *J. AOAC Int.* **2013**, *96*, 1372–1376.
38. Pieri, C.; Marra, M.; Moroni, F.; Recchioni, R.; Marcheselli, F. Melatonin: A peroxy radical scavenger more effective than vitamin E. *Life Sci.* **1994**, *55*, PL271–PL276.
39. Tan, D.X. Melatonin: A potent, endogenous hydroxyl radical scavenger. *Endocr. J.* **1993**, *1*, 57–60.



© 2020 by the authors. Licensee MDPI, Basel, Switzerland. This article is an open access article distributed under the terms and conditions of the Creative Commons Attribution (CC BY) license (<http://creativecommons.org/licenses/by/4.0/>).